Emirati Journal of Civil Engineering and Applications
Vol 2 Issue 2 (2024)
Pages (4 - 11)

Available at www.emiratesscholar.com

A Comparative Analysis of Thin-Walled Sections Using Finite Element Modelling

Fayiz Amin [1], Yasir Zaman[2], Abdul Wahid Anwar [1], Muhammad Asif [3], Khan Abdul Majid [3], Niazi Ehsanullah, [4]
Hafiz Ahmed Waqas[1]
fayizamin092@gmail.com, iamyasirzaman@gmail.com, asifkmuhammad123@gmail.com, abdulmajidk693@gmail.com, ahsanniazi@qq.com, wahid23421@gmail.com, hafiz.waqas@giki.edu.pk
Faculty of Civil Engineering, Ghulam Ishaq Khan Institute, Topi 23460, Pakistan.[1]
Faculty of Mechanical Engineering, Ghulam Ishaq Khan Institute, Topi 23460, Pakistan.[2]
Xi'an University of Technology, Shaanxi, Xi'an, Beilin, Jinhua S Rd, 710048, China.[3]
China three gorges University Yichang hubei.[4]

ARTICLE INFO

Published on 7th of August 2024
Doi: 10.54878/c87rtz38

KEYWORDS

Thin-Walled Sections, Folded Section, C-Section, Z-Section, FEM Modeling, ABAQUS

HOW TO CITE

A Comparative Analysis of Thin-Walled Sections Using Finite Element Modelling. (2024). Emirati Journal of Civil Engineering and Applications, 2(2), 4-11.

ABSTRACT

Thin-walled channel sections, such as Folded Sections, C-Sections, and Z-Sections, are extensively used in structural applications, particularly in civil engineering. This research investigates the behavior of cold-formed steel sections, including folded flanges, C-sections, and Z-sections, with respect to their ultimate load-carrying capacities. A numerical model will be developed using the finite element method in Abaqus software to simulate the behavior of these sections under axial compressive loading, covering both the elastic and plastic ranges. Comparative analysis of the folded sections, C-sections, and Z-sections is conducted. Z-section stands out with its significantly higher ultimate load capacity compared to the folded and C-sections. This can be attributed to its Z-shaped design. The objective of this study is to establish more robust design guidelines for the safe and efficient use of these sections in building structures. The findings will contribute to enhancing the reliability and economy of design practices for these structural elements.

1. Introduction

Thin-walled sections are structural elements with a wall thickness much smaller than other dimensions, often used in engineering and construction due to their efficient strength-to-weight ratio [1]. These sections, such as beams [2], columns [3], and frames [4], are prevalent in buildings and bridges, where minimizing weight while maintaining structural integrity is crucial. Their ability to withstand significant loads and resist buckling makes them essential in modern architecture and transportation, contributing to safer, more efficient, and cost-effective designs in everyday infrastructure and technology [5], [6], [7].

J.P. Papangelis et al. [8] examine stress and failure modes in thin-walled structures, focusing on cross-section and elastic buckling analyses. Their work includes calculating section properties, warping displacements, and longitudinal and shear stresses for thin-walled open and closed cross-sections of various geometries. Cao H. Pham et al. [9] used spline finite strip analysis to determine the buckling behavior of thin-walled steel channel sections (with and without lips) subjected to shear forces parallel to the web. They investigated the effects of flange width, boundary conditions, shear distribution, and length-to-width ratio on the critical buckling stresses, comparing results to existing solutions. T.A. Stone et al. [10] tested the behavior of built-up cold-formed steel studs made from two C-sections joined back-to-back. They found that current design standards for these studs used in walls and multi-story buildings might be overly conservative in predicting their load capacity.

Y.B. SudhirSastry et al. [11] analyzed the buckling behavior of thin-walled cold-formed beams under pure bending. They compared predicted buckling loads to published results, finding good agreement. The study investigated how beam dimensions (length, flange radius/thickness, extended flange length) affect buckling resistance. Beams with extended flanges showed the highest buckling loads, but rounded sections were deemed more efficient considering material and manufacturing costs. Cao Hung Pham et al. [12] investigates how holes (both circular and square) affect the shear buckling behavior of thin-walled channel sections with lips. They use the Spline Finite Strip Method (SFSM) to compare buckling of perforated plates and channels with centrally located holes, validating the method against the Finite Element Method (FEM). K.J.R. Rasmussen et al. [13] study compares different methods for analyzing the non-linear behavior of thin-walled channel columns under compression. They found good agreement between theoretical predictions and test results, particularly when local buckling occurred on the web. The paper also explores combining elastic and plastic analysis methods to describe the full load-bearing behavior of these columns.

Maria Kotełko et al. [14] explores the collapse behavior and load capacity of thin-walled structures, including box-section girders and channel-section beams. It combines theoretical analysis with experiments to examine the impact of material properties and cross-sectional shapes on collapse mechanisms. The study concludes by highlighting the influence of strain hardening and the effectiveness of various methods for estimating load-carrying capacity. Russell Q Bridge et al. [15] explores a series of tests on thin-walled steel tubes under axial load, investigating how tube dimensions and internal restraint affect buckling behavior. It examines a wide range of width-to-thickness ratios and explores methods to influence buckling mode. The results are compared to existing design standards and recommendations for improvement are proposed. R.F. Vieira et al. [16] present a novel one-dimensional modeling approach for the analysis of thin-walled structural systems. Unlike conventional models, this new methodology accounts for both the warping and bending deformation modes of the structure's cross-section, enabling a more accurate representation of the true three-dimensional behavior observed in real-world applications. The model achieves this enhanced accuracy through the implementation of a distinctive displacement approximation technique and a specialized method to delineate the various deformation patterns inherent to the system.

N. Silvestre et al. [17] explores the "distortional" mechanics of thin-walled sections, defining relevant cross-sectional properties and presenting a procedure to determine their distortional displacement field. The proposed method is validated through a C-section example, demonstrating good agreement with established numerical estimates. S. Al-Mosawi et al. [18] introduce an algorithm to optimize the cross-sections of cold-formed steel beams subjected to various loading conditions. The proposed approach effectively handles the impacts of diverse beam shapes and warping effects on the resulting stresses, solving the inherent non-linear problem through the application of an optimality criteria method. The study by H.R. Ronagh et al. [19] expands the analysis of

thin-walled beam-column structures to include tapered sections. The researchers derive expressions for non-linear axial strain and Kirchhoff stress resultants in these tapered configurations. This work lays a foundation for conducting finite element analysis of these structures and demonstrates consistency with previous research on specific tapered beam-column geometries.

The study conducted by Zbigniew Kowal et al. [20] investigates the critical loads that lead to local buckling in Z-section bars subjected to warping torsion. Through experiments on simply supported models, the researchers identified a specific "local ordered deflection interval" that enabled accurate determination of the buckling mode. Furthermore, the observed bimoment values, which are critical for the onset of buckling, were found to be dependent on the direction of the applied torsional load. The experimental findings were then compared against theoretical predictions. John T. Merrick et al. [21] investigates distortional buckling in cold-formed channel and Z-shaped structural members subjected to combined bending and torsional loads. It introduces general mathematical expressions to estimate the elastic distortional buckling stress for sections with return lips, including those with intricate geometries. The accuracy of these analytical formulas is verified through finite strip buckling analysis, and the researchers also provide explicit equations for the relevant flange properties.

2. Methodology

The research approach involves the modeling and analysis of section designs, including folded flanges, C-sections, and Z-sections, using the ABAQUS finite element software. This process includes incorporating detailed geometric characteristics, material properties, loading conditions, boundary constraints, and meshing techniques. A comparative evaluation is subsequently conducted to assess the ultimate load-bearing capacities of these distinct cross-section configurations. The study concludes with the validation and comparative assessment of the obtained results.

3. Geometry Details

The proposed cross-section configurations, including a channel section with folded section, a C-section, and a Z-section with limited thickness in one direction, were modeled using shell elements within the ABAQUS finite element software. The 2D drawing dimensions of these cross-sections are outlined in Figure 1.

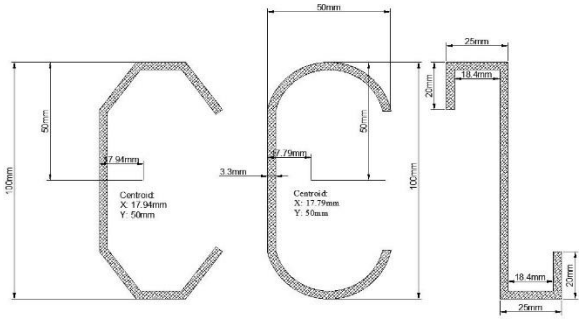

Figure1: 2D drawing of (a) Folded Section (b) C-Section (c) Z-Section

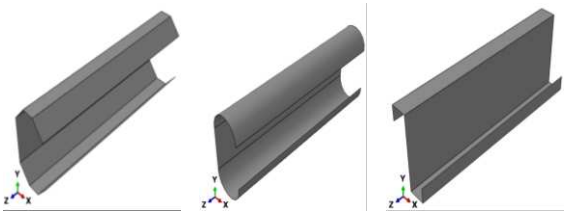

Figure2: 3D drawing of (a) Folded Section (b) C-Section (c) Z-Section

4. Material Properties

The material properties used in the Abaqus simulations for this study are those of ASTM A36 steel, a widely used structural steel known for its favorable characteristics such as excellent weldability [22], machinability [23], and relatively high strength [24]. Table 1 provides the specific material properties of the section under investigation [25].

Properties	ASTM A36 Steel
Elastic Modulus (GPa)	210
Poisson's ratio	0.3
Yield Strength (MPa)	250
Ultimate Strength (MPa)	400

Table 1 Material Properties of the ASTM A36 Steel

Additionally, Figure 3 depicts the stress-strain curve for ASTM A36 steel.

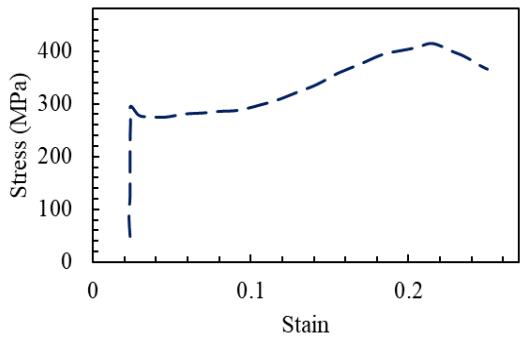

Figure 3: Stress Strain Curve of ASTM A36 Steel

5. Loading and Boundary Conditions

The sections were axially loaded through their centroid node, with the displacement applied using displacement control. At the unloaded end, translations in the x, y, and z directions, as well as rotation along the section length, were constrained, while rotations around the vertical and horizontal moment inertia axes were permitted. At the loaded end, translations along the section axis and rotation about the longitudinal profile's axis were restrained, but rotations around the major and minor axes, moment inertia axes, and longitudinal translation were allowed. A tie constraint was used to connect the plate and column ends, with the beam as the slave element and the column top end as the master element, and vice versa at the bottom end. The loading and boundary conditions for the different sections are depicted in Figure 4.

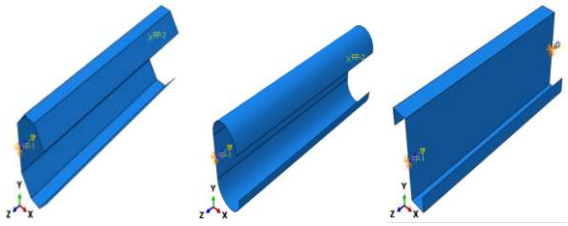

Figure 4: Loading and Boundary Conditions of (a) Folded Section (b) C-Section (c) Z-Section

6. Meshing

When the section thickness is less than one-tenth of a characteristic dimension, shell elements are appropriate for modeling. ABAQUS offers an extensive library of shell elements, including general-purpose, thin, and thick shell elements, which facilitate curved modeling, shell intersection, and nonlinear material response. To ensure accuracy, the element meshes were refined iteratively until an acceptable converged solution was achieved. In this study, a mesh size of 5 mm was adopted for all three models. Figure 5 illustrates the meshing of the models.

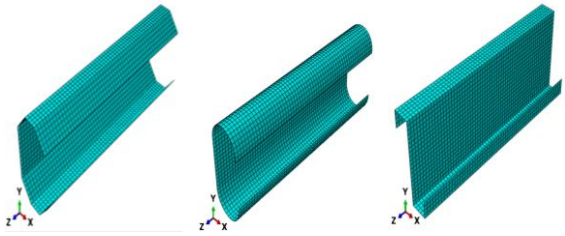

Figure 5: Meshing of (a) Folded Section (b) C-Section (c) Z-Section

7. Results and Discussion

7.1. FEM Results of the Sections

The failure morphology of the folded, C, and Z sections was examined. The folded and C sections exhibited local web buckling failure occurring at the mid-height. In contrast, the Z section displayed failure modes involving local buckling in the web along with flanges, also at the mid-height of the section. These findings, derived from finite element analysis (FEA), offer insights into the failure behavior and locations for each section. Figure 6 illustrates the failure morphology of the different sections.

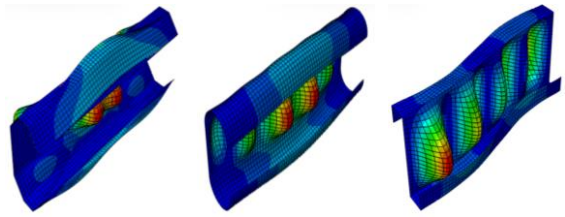

Figure 6: Failure Morphology of (a) Folded Section (b) C-Section (c) Z-Section

The Force Vs Axial shortening curve for the folded section Figure 7(a) reveals several key aspects of its

behavior under axial compression. The initial portion exhibits a linear trend, indicating elastic deformation according to Hooke's Law. However, pinpointing a distinct yield point is challenging due to limited data points around the expected yield stress of ASTM A36 steel. After this initial stage, the curve shows a gradual decrease in slope, signifying plastic deformation where the material experiences permanent strain under increasing load. The peak of the curve represents the folded section's ultimate load capacity, the maximum force it can withstand before failure. Notably, the graph shows a sharp drop in load after the peak, suggesting a sudden and potentially brittle failure mode. This behavior could be attributed to buckling at the fold location, a vulnerability inherent to the folded geometry. While the C-section's curve Fig. 7(b) resembles the folded section's behavior but with a possible stiffness advantage. Its closed web might provide greater initial resistance to compression (steeper slope). However, the open web is vulnerable to buckling. While the post-peak behavior needs more data, it might indicate a less brittle failure compared to the folded section.

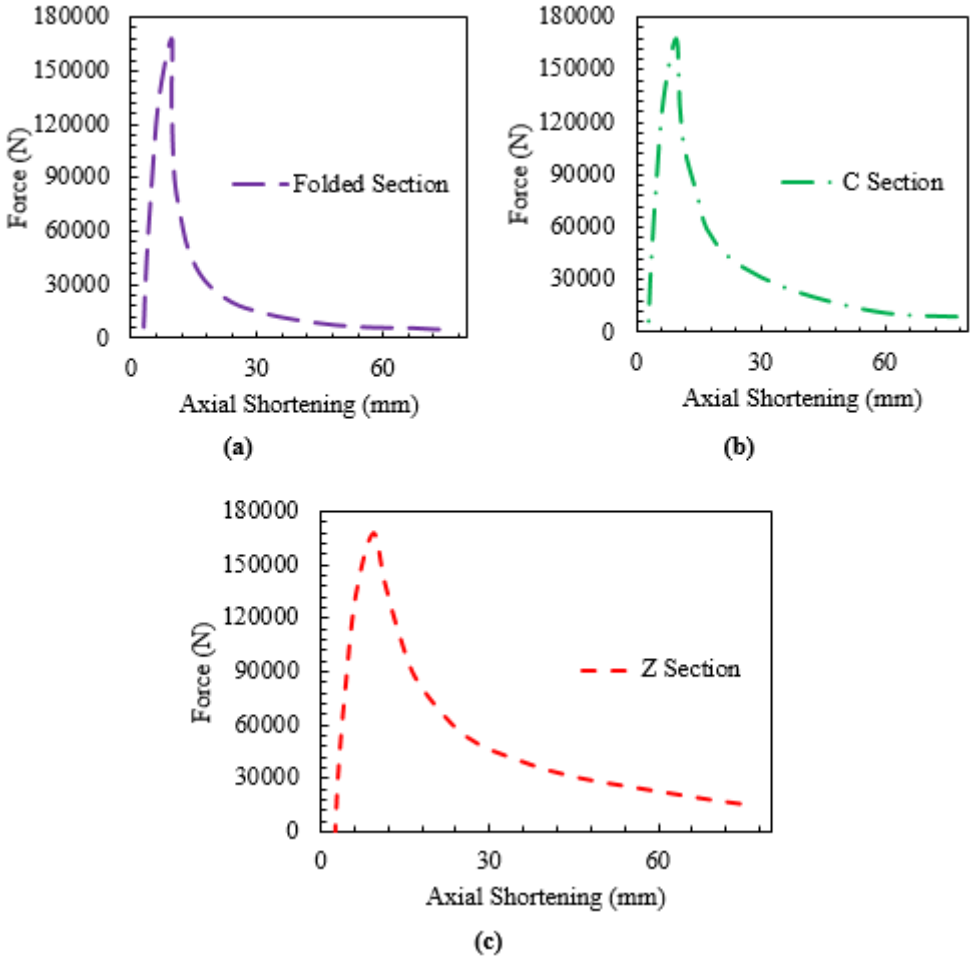

Figure7: (a) Force VS Axial Shortening of Folded Section (b) Force VS Axial Shortening of C Section

The Z-section's curve Figure 7(c) reinforces its superior performance under axial compression. Like the other sections, it exhibits an initial linear elastic region followed by plastic deformation. Identifying a distinct yield point remains challenging. However, the Z-section stands out with its significantly higher ultimate load capacity compared to the folded and C-sections. This can be attributed to its Z-shaped design,

which efficiently distributes material and potentially leads to a higher moment of inertia. This allows the Z-section to resist bending induced by axial compression more effectively. The post-ultimate behavior also appears more ductile compared to other sections, evident by a more gradual decrease in load after reaching the peak. This suggests the Z-section can sustain some load even after surpassing its ultimate capacity

7.2. Results Comparison of Sections

The numerical simulations revealed distinct load-carrying behaviors amongst the investigated thin-walled sections (folded, C, and Z) under axial compression. As anticipated, the Z-section exhibited the superior ultimate load capacity compared to the folded and C-sections. This superior performance can be attributed to the Z-section's unique geometric design. The presence of flanges on both sides, combined with the web, provides a more efficient distribution of material compared to the open web of the C-section and the folded geometry. This enhanced distribution likely results in a higher moment of inertia for the Z-section, allowing it to resist bending induced by axial compression more effectively. The folded section's performance was the most limited due to the potential for localized buckling at the fold location.

The comparison graph further corroborated these observations. All sections exhibited a linear load-displacement relationship in the initial stages, signifying elastic behavior according to Hooke's Law. This linearity persisted until approximately 75% of the ultimate load was reached. Beyond this point, the behavior transitioned into the post-buckling range, evident in Figure 8. Here, non-linear behavior dominated, with the load increasing gradually at a slower rate while the end-shortening experienced rapid growth. This stage corresponds to the sections' decreasing ability to resist deformation. Upon reaching the ultimate load, the stub columns failed and lost their capacity to bear additional loads. Consequently, the load curves declined as the end-shortening exceeded the ultimate load.

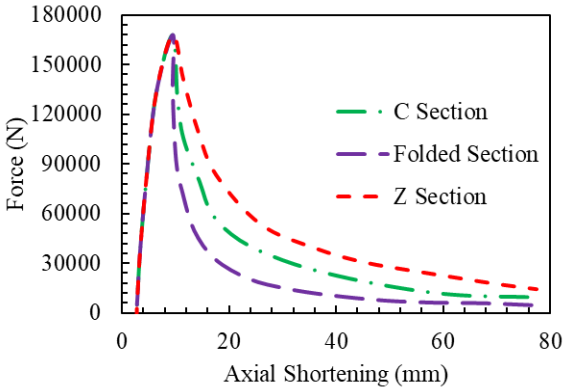

Figure 8: Results Comparison of all Sections

8. Conclusion

This study employed comparative analysis of thin-walled sections using finite element modeling of proposed configurations such as folded flanges, C-sections, and Z-sections. Numerical techniques were utilized to apply axial compressive loads to each section, incorporating specific boundary conditions and interactions. The results indicate that vertical and lateral deformations remained minimal until the ultimate load was exceeded, at which point deformations became significant. The Z-section exhibited superior load-carrying capacity compared to other sections, attributed to its unique geometric design and structural properties. Its capability to withstand higher loads before failure positions it favorably for applications requiring robust compression load-bearing capabilities, potentially enhancing the structural integrity of diverse engineering projects. Future research endeavors could concentrate on refining the design and dimensions of the Z-section to optimize its load-bearing potential across varied structural systems. Here are some future recommendations for further study and application of thin-walled sections.

- Material Optimization and Behavior: Investigate the effect of different materials, including advanced alloys or composites, on the load-carrying capacity and deformation behavior of thin-walled sections.
- Dynamic Loading Conditions: Explore the response of thin-walled sections under dynamic loading conditions, such as impact or seismic loads.

- Environmental Effects and Sustainability: This could involve life cycle assessments (LCAs) to evaluate energy consumption, carbon footprint, and recyclability, aiming to optimize designs for eco-friendly and cost-effective solutions.

References

1. N. S. Ha and G. Lu, "Thin-walled corrugated structures: A review of crashworthiness designs and energy absorption characteristics," Thin-Walled Structures, vol. 157, p. 106995, Dec. 2020, doi: 10.1016/J.TWS.2020.106995.
2. O. Bourihane, A. Ed-Dinari, B. Braikat, M. Jamal, F. Mohri, and N. Damil, "Stability analysis of thin-walled beams with open section subject to arbitrary loads," Thin-Walled Structures, vol. 105, pp. 156–171, Aug. 2016, doi: 10.1016/J.TWS.2016.04.008.
3. D. C. Han and S. H. Park, "Collapse behavior of square thin-walled columns subjected to oblique loads," Thin-Walled Structures, vol. 35, no. 3, pp. 167–184, Nov. 1999, doi: 10.1016/S0263-8231(99)00022-1.
4. Dica. - and G. Gabbianelli Advisor Armando Gobetti Revisor Profssa Lucia Faravelli, "Numerical model for framed structures with thin-walled cross-section members," Dec. 2017, Accessed: Jul. 09, 2024. [Online]. Available: https://iris.unipv.it/handle/11571/1203323
5. M. W. Hilburger, "Buckling of Thin-Walled Circular Cylinders." 2020.
6. Q. Al-Kaseasbeh and I. H. P. Mamaghani, "Buckling Strength and Ductility Evaluation of Thin-Walled Steel Tubular Columns with Uniform and Graded Thickness under Cyclic Loading," Journal of Bridge Engineering, vol. 24, no. 1, p. 04018105, Jan. 2018, doi: 10.1061/(ASCE)BE.1943-5592.0001324.
7. T. T. Nguyen, P. T. Thang, and J. Lee, "Lateral buckling analysis of thin-walled functionally graded open-section beams," Compos Struct, vol. 160, pp. 952–963, Jan. 2017, doi: 10.1016/J.COMPSTRUCT.2016.10.017.
8. J. P. Papangelis and G. J. Hancock, "Computer analysis of thin-walled structural members," Comput Struct, vol. 56, no. 1, pp. 157–176, Jul. 1995, doi: 10.1016/0045-7949(94)00545-E.
9. C. H. Pham and G. J. Hancock, "Shear buckling of thin-walled channel sections," J Constr Steel Res, vol. 65, no. 3, pp. 578–585, Mar. 2009, doi: 10.1016/J.JCSR.2008.05.015.
10. T. A. Stone and R. A. LaBoube, "Behavior of cold-formed steel built-up I-sections," Thin-Walled Structures, vol. 43, no. 12, pp. 1805–1817, Dec. 2005, doi: 10.1016/J.TWS.2005.09.001.
11. Y. B. Sudhirsastry, Y. Krishna, and P. R. Budarapu, "Parametric studies on buckling of thin-walled channel beams," Comput Mater Sci, vol. 96, no. PB, pp. 416–424, Jan. 2015, doi: 10.1016/J.COMMATSCI.2014.07.058.
12. C. H. Pham, "Shear buckling of plates and thin-walled channel sections with holes," J Constr Steel Res, vol. 128, pp. 800–811, Jan. 2017, doi: 10.1016/J.JCSR.2016.10.013.
13. K. J. R. Rasmussen and G. J. Hancock, "Nonlinear analyses of thin-walled channel section columns," Thin-Walled Structures, vol. 13, no. 1–2, pp. 145–176, Jan. 1992, doi: 10.1016/0263-8231(92)90006-I.
14. M. Kotełko, "Load-capacity estimation and collapse analysis of thin-walled beams and columns—recent advances," Thin-Walled Structures, vol. 42, no. 2, pp. 153–175, Feb. 2004, doi: 10.1016/S0263-8231(03)00055-7.
15. R. Q. Bridge and M. D. O'Shea, "Behaviour of thin-walled steel box sections with or without internal restraint," J Constr Steel Res, vol. 47, no. 1–2, pp. 73–91, Aug. 1998, doi: 10.1016/S0143-974X (98)80103-X.
16. R. F. Vieira, F. B. Virtuoso, and E. B. R. Pereira, "A higher order model for thin-walled structures with deformable cross-sections," Int J Solids Struct, vol. 51, no. 3–4, pp. 575–598, Feb. 2014, doi: 10.1016/J.IJSOLSTR.2013.10.023.
17. N. Silvestre and D. Camotim, "On the mechanics of distortion in thin-walled open sections," Thin-Walled Structures, vol. 48, no. 7, pp. 469–481, Jul. 2010, doi: 10.1016/J.TWS.2010.02.001.
18. S. Al-Mosawi and M. P. Saka, "Optimum shape design of cold-formed thin-walled steel sections," Advances in Engineering Software, vol. 31, no. 11, pp. 851–862, Nov. 2000, doi: 10.1016/S0965-9978(00)00047-8.
19. H. R. Ronagh, M. A. Bradford, and M. M. Attard, "Nonlinear analysis of thin-walled members of variable cross-section. Part I: Theory," Comput Struct, vol. 77, no. 3, pp. 285–299, Jun. 2000, doi: 10.1016/S0045-7949(99)00223-0.
20. Z. Kowal and A. Szychowski, "Experimental determination of critical loads in thin-walled bars with Z-section subjected to warping torsion," Thin-Walled Structures, vol. 75, pp. 87–102, Feb. 2014, doi: 10.1016/J.TWS.2013.10.020.

21. J. Merrick, G. Hancock, and M. Bamach, "Distortional Buckling Formulae for Thin-Walled Channel and Z-sections with Return Lips," CCFSS Proceedings of International Specialty Conference on Cold-Formed Steel Structures (1971 - 2018), Oct. 1998, Accessed: Jul. 09, 2024. [Online]. Available: https://scholarsmine.mst.edu/isccss/14iccfsss/14iccfsss-session1/3
22. K. Buranapunviwat and K. Sojiphan, "Destructive testing and hardness measurement of resistance stud welded joints of ASTM A36 steel," Mater Today Proc, vol. 47, pp. 3565–3569, Jan. 2021, doi: 10.1016/J.MATPR.2021.03.562.
23. S. A. Afolalu et al., "Impact of heat treatment on HSS cutting tool (ASTM A600) and its behaviour during machining of mild steel (ASTM A36)," AIP Conf Proc, vol. 1957, no. 1, p. 50003, Apr. 2018, doi: 10.1063/1.5034333/737966.
24. H. Chen, G. Y. Grondin, and R. G. Driver, "Characterization of fatigue properties of ASTM A709 high performance steel," J Constr Steel Res, vol. 63, no. 6, pp. 838–848, Jun. 2007, doi: 10.1016/J.JCSR.2006.08.002.
25. G. Beulah, G. Ananthi, S. Vishuvardhan, and S. Knight, "Experimental, theoretical and numerical study on thin-walled steel single and compound channel sections in axial compression," IJEMS Vol.22(5) [October 2015], vol. 22, pp. 570–580, 2015, Accessed: Jul. 10, 2024. [Online]. Available: http://nopr.niscpr.res.in/handle/123456789/33440